

## Electron density measurement by differential interferometry

W. X. Ding, D. L. Brower, B. H. Deng, and T. Yates

*Electrical Engineering Department, University of California-Los Angeles, Los Angeles, California 90095*

(Received 5 May 2006; presented on 10 May 2006; accepted 16 June 2006; published online 26 September 2006)

A novel differential interferometer is being developed to measure the electron density gradient and its fluctuations. Two separate laser beams with slight spatial offset and frequency difference are coupled into a single mixer making a heterodyne measurement of the phase difference which is <1% of the total phase change experienced by each beam separately. This measure of the differential phase is made at multiple spatial points and can be inverted directly to provide the local density distribution. © 2006 American Institute of Physics. [DOI: 10.1063/1.2229217]

### I. INTRODUCTION

A high-speed vertically viewing multichord heterodyne far-infrared (FIR) laser interferometer system has been employed on the MST reversed field pinch (RFP) to measure the electron density profile for many years.<sup>1</sup> Using a conventional approach, a probe beam is mixed with a local oscillator (LO) beam for each chord and the change in phase with respect to a reference signal is measured giving the line-integrated density. Recently, we have modified the MST interferometer system by utilizing two slightly offset probe beams with different frequency  $\sim 1$  MHz to directly measure the phase difference for the separate paths. In this new configuration, referred to as a differential interferometer, the system is insensitive to path length changes due to vibrations and thermal expansion effects since both probing beams traverse nearly identical optical paths and use the same optical elements including mixer. In addition, the measured phase difference can be controlled, by varying the spatial offset, and set to  $< 2\pi$  eliminating the potential for fringe counting errors. The differential interferometer approach is applicable to any fusion device including ITER and its divertor where the dynamic range of density is large and machine vibrations and thermal expansion are expected to be severe.

To illustrate the principle of the differential interferometer, we start with a conventional interferometer where the plasma-induced phase change in a cylindrical geometry is given by

$$\phi(x) = r_e \lambda \int_{-\sqrt{a^2-x^2}}^{\sqrt{a^2-x^2}} n_e(r) dz, \quad (1)$$

where  $r_e = 2.82 \times 10^{-15}$  m is the classical radius of electron,  $\lambda$  is the laser wavelength,  $z$  is the distance along the chord,  $x$  is the impact parameter and  $x^2 + z^2 = r^2$ . The density profile is found by performing a standard Abel inversion<sup>2</sup> using

$$n_e(r) = -\frac{1}{\pi r_e \lambda} \int_r^a \frac{\partial \phi(x)}{\partial x} \frac{dx}{\sqrt{x^2 - r^2}}. \quad (2)$$

From this relation it is clear that the first spatial derivative of the phase,  $\partial \phi / \partial x$ , is required to obtain  $n_e(r)$ . Conventional

interferometers measure  $\phi(x)$  for multiple discrete chords, make a numerical fit to the available points, take the spatial derivative to infer  $\partial \phi / \partial x$ , and then perform an inversion. The difficulty in directly measuring  $\partial \phi / \partial x$  is that the phase difference becomes smaller as two adjacent chords are brought closer together. However, phase noise due to vibrations and other effects also becomes smaller since both probe beams see similar optical paths. By taking advantage of the reduced phase noise, measurement of small phase difference becomes feasible. This fact motivates us to devise a scheme to directly measure  $\partial \phi / \partial x$  at multiple spatial points and then invert to obtain the local density profile. Herein, we will describe the differential interferometer measurement method, present results from initial tests, and discuss the advantages and limitations of this novel density measurement technique.

### II. EXPERIMENTAL SETUP

The differential interferometer system employed on MST utilizes two parallel, linearly polarized, spatially offset FIR laser beams ( $\lambda = 432 \mu\text{m}$ ) with frequency difference  $\sim 1$  MHz to probe the plasma at each chord position ( $x$ ), as shown in Fig. 1. Other relevant details of the system hardware have been described elsewhere.<sup>3</sup> The two parallel laser beams are initially slightly offset a small distance ( $\delta$ ) and then divided into 11 separate chords by wire mesh beam splitters. The phase difference between these two probing beams at each chord position with respect to a reference signal is obtained directly using a digital phase comparator technique<sup>4</sup> in order to determine  $\Delta \phi(x, t)$ . In this configuration, the system has a fast time response,  $\sim 1 \mu\text{s}$ , and phase noise less than  $0.05^\circ$  for a 20 kHz bandwidth. A third FIR laser (also frequency offset) serves as LO for each mixer to permit simultaneous measurement of  $\phi(x, t)$  via the conventional approach. This information can be used for comparison and calibration purposes, as will be shown later.

### III. EXPERIMENTAL RESULTS

The first test of the 11 chord differential interferometer has been performed on the MST RFP, a circular cross section device with major radius  $R = 1.5$  m, minor radius  $a = 0.52$  m,

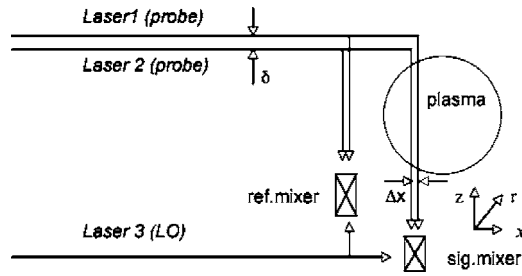


FIG. 1. Schematic of the differential interferometer experimental setup. Note that beam offsets at the source ( $\delta$ ) and in the plasma ( $\Delta x$ ) are different due to an optical system with out-of-plane non-45° bends that are not pictured.

discharge current  $I_p \leq 600$  kA, line-averaged electron density  $n_e \sim 1 \times 10^{19} \text{ m}^{-3}$ , and electron temperature  $T_e \leq 1$  keV.

Differential interferometer time series data for each chord position are shown in Fig. 2 for  $\delta=3.5$  mm. No fringe counting errors are observed as the maximum phase change is  $< 5^\circ$ . In this figure, the bandwidth is limited to 20 kHz and the rms noise level is about  $\sim 0.05^\circ$ . This compares very favorably to the conventional interferometer setup where the rms noise level is  $1^\circ$ – $2^\circ$ . For each rapid sawtooth crash ( $< 200 \mu\text{s}$ ) shown in Fig. 2(a), the differential interferometer clearly tracks the fast density dynamics, as shown in Figs. 2(b) and 2(c). High-frequency fluctuations superimposed on the equilibrium density traces are associated magnetic fluctuations (tearing instabilities). Initially, the two probe beams are made collinear (i.e.,  $\delta=0$ ) so that the phase difference is minimized ( $\Delta\phi \sim 0$ ), as shown in Fig. 3(a) (open circles). Then, one probe beam is spatially offset ( $\delta=3.5$  mm) by translating a mirror while keeping the two beams parallel. With this orientation, the phase change for the central chords remains unchanged but a nonzero phase difference is measured for the edge chords, as shown in Fig. 3(a) (solid

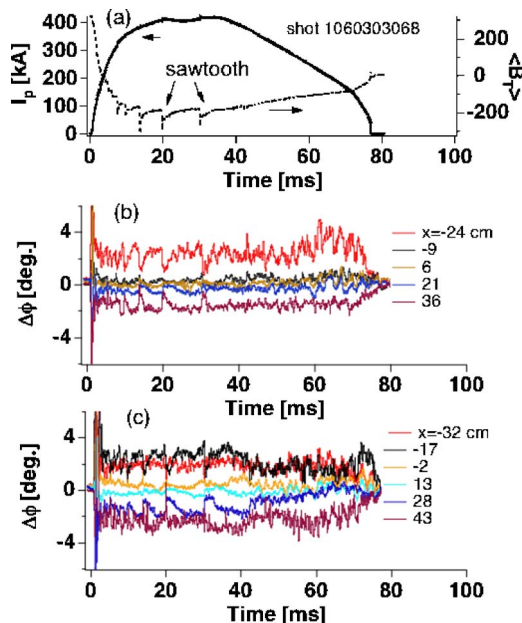


FIG. 2. (a) Time history of discharge current and average toroidal magnetic field. The arrows point to sawtooth crashes. [(b) and (c)] Time history of the differential interferometer for 11 chords where  $x$  denotes the impact parameter of the laser beams and  $\delta=3.5$  mm.

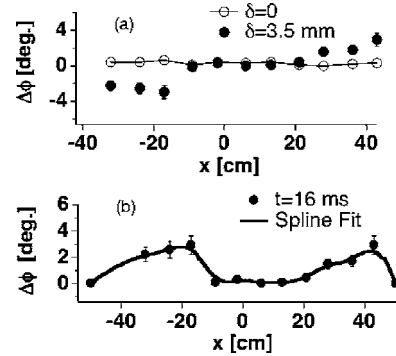


FIG. 3. (a) Phase difference profile with separations  $\delta \sim 0$  (open circles) and  $\delta \sim 3.5$  mm (solid circles); (b) spline fit to measured  $|\Delta\phi|$  profile used for inversion.

circles). This is expected since the density gradient is small in the plasma core and large in the edge. In addition, the phase gradient (or phase difference between two adjacent beams) changes the sign across the magnetic axis consistent with the sign change of the density gradient.

It is important to note that the effective separation of two beams in the plasma ( $\Delta x$ , in radial direction) is not equal to  $\delta$ . There is also a toroidal displacement of two probe beams resulting from an optical system more complicated than shown schematically in Fig. 1. Density variation resulting from toroidal offset is negligible. Maintaining small beam separation is crucial to measuring  $\partial\phi/\partial x$  and achieving maximum vibration reduction by use of a single mixer. However, it is difficult to physically measure this offset because it is small compared to the beam diameter of  $\sim 1$  cm.

As opposed to making a direct measurement of the separation, an alternate method has been developed to absolutely determine the effective offset of the beams by calibrating the differential interferometer using the conventional interferometer. Since the probe beams are offset by a known amount  $\delta$  before splitting into 11 chords, we take the separation  $\Delta x$  of two beams in the plasma for each chord to be identical. In addition, we assume  $\Delta x = k\delta$ , where  $k$  is a calibration constant to be experimentally determined. As mentioned earlier, one can obtain the local density profile by measuring the phase gradient  $\Delta\phi/\Delta x$  and performing an inversion. Before inversion, a spline fit is made to the absolute value of the differential phase profile,  $|\Delta\phi|$ , as shown in Fig. 3(b). The boundary condition  $d\phi/dx=0$  is added at  $r=50$  cm. The uncalibrated density profile from the differential interferometer

$$n_e(r)|_\delta = -\frac{1}{\pi\lambda r_e} \int_r^a \frac{\Delta\phi(x)}{\delta} \frac{dx}{\sqrt{x^2 - r^2}} = k \times n_e(r)$$

is then obtained directly. In addition, the standard line-integrated density measurement, shown in Fig. 4, can also be used to find  $n_e(r)$ . Since the differential and conventional interferometers operate simultaneously, we can determine  $k$  from the relation  $r_e\lambda \int n_e(r)|_\delta dz = k\phi(x)$ , where  $\phi(x)$  is the phase measured by the conventional interferometer, as shown in Fig. 5(a) at  $t=16$  ms. Using this approach, we find  $k=0.35$  making the effective separation of two beams  $\Delta x = 1.20$  mm. Once  $k$  is known, the differential interferometer

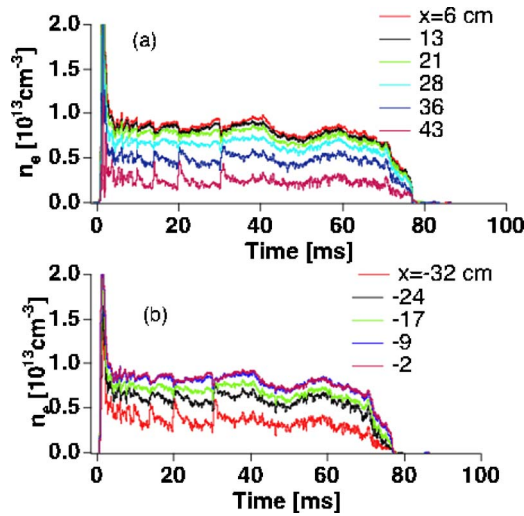


FIG. 4. Time history of line-averaged electron density for 11 chords measured using conventional interferometry (same shot as Fig. 2).

can be used independently to determine  $n_e(r)$  for any discharge.

The phase gradient  $\Delta\phi/\Delta x$  from the differential interferometer measurement is shown in Fig. 5(b). This same parameter can also be obtained numerically by fitting  $\phi(x)$  [in Fig. 5(a)] and taking the derivative as plotted in Fig. 5(b). Both give consistent results within experimental errors. This agreement confirms the assumption that  $k$  is constant for the 11 chords. For purposes of comparison, the density profiles obtained using the conventional interferometer and differential interferometer measurements at time  $t=16$  ms are shown in Fig. 5(c). The agreement is not surprising since the two interferometric techniques produced the same  $\Delta\phi/\Delta x$  profile.

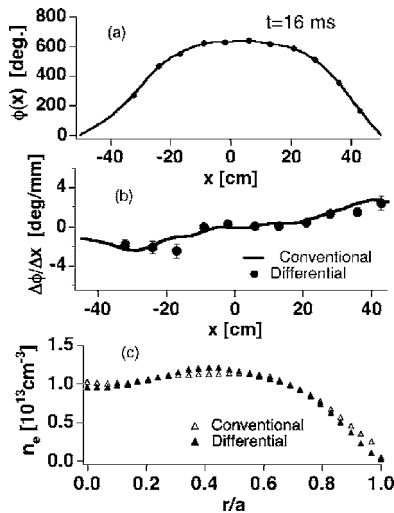


FIG. 5. (a) Measured phase profile  $\phi(x)$  at  $t=16$  ms for conventional interferometer (solid circles); the solid line is spline fit to measured points; (b) first derivative of phase,  $d\phi/dx$ , is calculated and shown as solid line. The direct measurements from differential interferometer are shown by solid circles using  $\Delta x=1.20$  mm; (c) density profile comparison using the conventional and differential interferometer techniques.

## IV. DISCUSSION AND SUMMARY

Mathematically, determination of density profile from measurements of  $\phi(x)$  or  $d\phi/dx$  are equivalent as shown by the simple relation  $\phi(x)=\sum_i(\partial\phi/\partial x_i)\Delta x_i$ , which is valid for a multichord interferometer. However, technically, the differential interferometer has some distinct advantages over the conventional interferometer approach. The total phase change measured by an interferometer can be written as

$$\phi(x) = r_e \lambda \int n_e(r) dz + \frac{2\pi}{\lambda} \delta L, \quad (3)$$

where  $\delta L$  represents the change in path length due to vibrations or thermal expansion. From this relation it is straightforward to see how the phase difference between two nearly collinear probe beams with small  $\Delta\lambda$  will be independent of  $\delta L$ . Consequently, the differential interferometer does not require vibration compensation like conventional interferometers. In addition, the optimum choice for  $\Delta x$  can be decided experimentally. If the probing beams are too close, the phase shift becomes small compared to system phase noise. Likewise, if the probing beams are too far apart, the total phase can become  $>2\pi$  or vibration effects can be reintroduced.

Unlike conventional interferometers, the differential interferometer is not affected by changes in path length. In addition, since the total plasma-induced phase change  $\ll 2\pi$ , it is immune to fringe counting errors providing a tremendous advantage for monitoring long pulse length discharges. Recovery from any temporary loss of signal due to plasma instability (ELM, minor disruption, etc.), or even source problems is possible without encountering multiple fringe ambiguities.

A new multichord differential interferometer has been successfully tested on MST to determine the electron density profile. The technique is insensitive to path length changes and measures a total phase difference less than 1% fringe. Differential interferometry essentially provides a local density gradient measurement due to the close chord spacing. This capability, along with the fast time response, will be exploited in the future to provide a direct measure of density gradient fluctuations. Optimization of differential interferometer technique is currently being pursued on MST and has potential application to a variety of fusion devices.

## ACKNOWLEDGMENTS

The authors gratefully acknowledge contributions from the MST group. This work is supported by the U.S. Department of Energy.

<sup>1</sup>S. R. Burns, W. A. Peebles, D. Holly, and T. Lovell, Rev. Sci. Instrum. **63**, 4993 (1992).

<sup>2</sup>I. H. Hutchinson, *Principles of Plasmas Diagnostics* (Cambridge University Press, New York, 2002).

<sup>3</sup>D. L. Brower *et al.*, Rev. Sci. Instrum. **74**, 1534 (2003).

<sup>4</sup>Y. Jiang, D. L. Brower, L. Zeng, and J. Howard, Rev. Sci. Instrum. **68**, 902 (1997).